catalysts

MDPI

Article

Effect of Preparation Conditions on Structure and Activity of Sodium-Impregnated Oyster Shell Catalysts for Transesterification

Han Jin [1], Praveen Kolar [1,*], Steven W. Peretti [2], Jason A. Osborne [3] and Jay J. Cheng [1]

[1] Department of Biological and Agricultural Engineering, North Carolina State University, Raleigh, NC 27695, USA; hjin4@ncsu.edu (H.J.); jcheng3@ncsu.edu (J.J.C.)
[2] Department of Chemical & Biomolecular Engineering, North Carolina State University, Raleigh, NC 27695, USA; peretti@ncsu.edu
[3] Department of Statistics, North Carolina State University, Raleigh, NC 27695, USA; jaosborn@ncsu.edu
* Correspondence: pkolar@ncsu.edu; Tel.: +1-919-513-9797

Received: 21 May 2018; Accepted: 21 June 2018; Published: 26 June 2018

Abstract: The catalyst preparation technique plays a significant role in its activity and durability. The present research investigated sodium hydroxide and sodium chloride as the precursor chemicals for impregnation on waste oyster shells that were tested as heterogeneous base catalysts for transesterification of soybean oil. Effects of precursor concentration and calcination temperature on the surface structure and the activity of the catalysts were studied via the one-factor-at-a-time method. The optimal impregnation concentrations of sodium hydroxide and sodium chloride were determined to be 6 mol/L and 2.43 mol/L, respectively. The optimal calcination temperature was determined to be 800 °C for both sodium hydroxide and sodium chloride-impregnated catalysts. Analyses of the catalysts via X-ray Diffraction and X-ray photoelectron spectroscopy indicated that different active species were formed on the surface depending on the calcination temperature. Results obtained from this study could be used to fine-tune the procedure for the synthesis of transesterification catalysts from aquatic animal shells.

Keywords: oyster shell; impregnation; transesterification; fatty acid methyl ester; biodiesel

1. Introduction

Solid base catalysts have been extensively studied for their catalytic performance in transesterification reactions [1]. CaO is one of such solid base catalysts capable of transesterification of various oils to fatty acid methyl esters (FAME). However, its activity was still found to be lower than that of NaOH [2]. Hence, to increase the catalytic activity of CaO, wet impregnation methods have been employed to modify the surface of CaO to generate more active sites. Doped could react with the oxygen present in CaO to produce defect sites on the surface, which served as the enhanced basic sites for transesterification reactions [3–8]. Watkins et al., impregnated CaO with a series of $LiNO_3$ solutions in the range of 1–20 wt. % [4]. Despite showing a continuous drop in specific surface area (with increasing Li content), all Li-impregnated CaO catalysts that were tested exhibited increased basic strengths when compared to CaO. The transesterification results indicated that the initial reaction rate increased with the increased Li content and reached a maximum when Li content reached 1.23 wt. %. Further, the characterization study indicated that the doped CaO helped the formation of surface OH^- which enhanced the catalytic activity. However, it was noted that the high concentration of $LiNO_3$ may have covered the surface OH^- group, and thus may have lowered the catalytic activity.

In addition to the alkali metal oxides and hydroxide groups generated from the impregnation-calcination method, calcium and halogen have also been identified by many research

groups as active species. Mar and Somsook used KCl to modify the surface of CaO by the wet impregnation method under microwave irradiation followed by calcination [5]. When the catalyst was characterized, $KCaCl_3$ phase was detected on the surface, which contributed to the increased FAME yield during transesterification of soybean oil using methanol. A similar observation has been reported by Wen et al., in which KF was tested as an impregnating agent on CaO [6]. A new $KCaF_3$ phase was observed on the surface of the catalysts and the increased catalytic activity was attributed to the higher H^+ affinity for F^-. Similarly, Liu et al., synthesized CsF/CaO catalyst by mixing CsF solution with $Ca(OH)_2$ solution followed by calcination [7]. The catalyst exhibited excellent activity in transesterification reaction in which about 98% FAME yield was obtained in 1 h under optimal reaction conditions. The highly improved activity was plausibly attributed to the formation of $CsCaF_3$ on the surface. Interestingly, somewhat different results were obtained when KBr was impregnated on CaO [8]. XRD analyses did not detect the presence of $KCaBr_3$ phase on the surface, perhaps because of the larger radius of Br that may not have allowed the formation of $KCaBr_3$ on the surface.

Besides alkaline metals, other chemical agents have also been tested for their ability to enhance the catalytic activity of CaO. Yan et al., synthesized a solid catalyst, Ca_3La_1, by mixing $La(NO_3)_3$ solution with $Ca(Ac)_2$ solution followed by addition of ethanol and bubbling the solution with CO_2.The resultant precipitate was calcined to obtain Ca_3La_1 [9]. The as-synthesized catalyst consisted of $Ca(OH)_2$ as the major phase on the surface, and the initial reaction rate and FAME yield after 2 h using Ca_3La_1 were similar to the NaOH-catalyzed transesterification, indicating Ca_3La_1 as a potential substitute for transesterification reactions. Kuar and Ali synthesized Zr/CaO catalyst using wet impregnation by mixing CaO with $ZrOCl_2 \cdot 8H_2O$ solution followed by calcination [10]. The 15 wt. % Zr/CaO calcined at 700 °C exhibited highest reaction rate in transesterifying jatropha curcas oil. The authors attributed the activity of the catalyst to the relatively lower ratio of tetragonal to monoclinic ZrO_2 on the surface and decreased crystallite size.

Recently, waste natural shells have attracted attention, since they could serve as the economical precursors for CaO. Various natural shells have been tested for catalyzing transesterification reactions. For example, Wei et al. used waste eggshell as the precursor for the catalyst and reported a FAME yield of over 95% during transesterification of soybean oil for a methanol to oil ratio (MR) of 9, and catalyst loading (CL) of 3%, at 65 °C within 3 h [11]. Rezaei et al., employed calcined mussel shell to catalyze transesterification of soybean oil and observed a 94.1% FAME yield at MR of 24, CL of 12% at 60 °C in 8 h [12]. Similarly, calcined capiz shell (Amusium cristatum) was tested as a catalyst for converting palm oil into FAME by Suryaputra et al., who reported a FAME yield of 93% using a MR of 8 and CL of 3% [13]. However, the natural shell-derived CaO exhibited relatively lower activity compared to commercial CaO and NaOH [11–13]. Thus, to improve the activity, natural shells may be impregnated with chemicals. Jaraim et al., improved the activity of calcined oyster shell by impregnating 1 mmol/g of KI [14]. Additionally, preparation conditions could be manipulated to enhance the activity of shells. Wei et al. investigated the effect of calcination temperature and reported that eggshells calcined at 800 °C or above exhibited high activity due to the formation of CaO [11]. Similar results were observed by Rezaeti et al., wherein the minimum calcination temperature was observed to be 950 °C for the formation of CaO [12].

In our recent research, we reported an active base catalyst that was prepared by impregnating NaOH on oyster shell followed by calcination [15]. Our results indicated that impregnation of NaOH on oyster shell increased the FAME yield from 71% (3 h reaction time) (control) to 87% (1 h reaction time). In addition, the analysis of the surface of the catalyst revealed that impregnation of NaOH followed by calcination resulted in the formation of sodium peroxide species that significantly enhanced the activity of the calcined oyster shells [16].

Further, the activity of the oyster shell catalyst directly depends on the preparation conditions, especially precursor loading, and calcination temperature. In other words, right amounts of precursor when calcined at right temperature will maximize the formation of active sites on the surface that can significantly enhance transesterification reactions. However, to our knowledge, there is limited

information on how the activity of oyster shell catalyst is influenced by preparation conditions. By elucidating how calcination temperature and impregnation conditions affect the catalyst activity will not only improve catalyst synthesis processes but also allow us to predict the performance of the catalyst. Hence, the goal of this research is to systematically investigate how the catalyst preparation conditions (precursor type, precursor concentration, calcination temperature) influence the structure and subsequent activity of the catalyst.

2. Results and Discussion

2.1. Effects of the Precursor Type and Concentration

Figure 1 summarized the effects of precursor type and concentration. For both precursors, the calcined oyster shell (COS) was used as a control for comparison purposes. When a concentration of 2 mol/L was used for impregnation, there were no significant differences between the FAME yields obtained from control (COS) and NaCl/shell and NaOH/shell catalysts suggesting that no catalytically active sites were formed on the surface of the oyster shells at lower precursor concentrations. When the precursor concentrations were increased, significant differences were observed. For NaOH/shell experiments, FAME yields increased from 8% to 83% when precursor (NaOH) concentration increased from 2 mol/L to 6 mol/L.

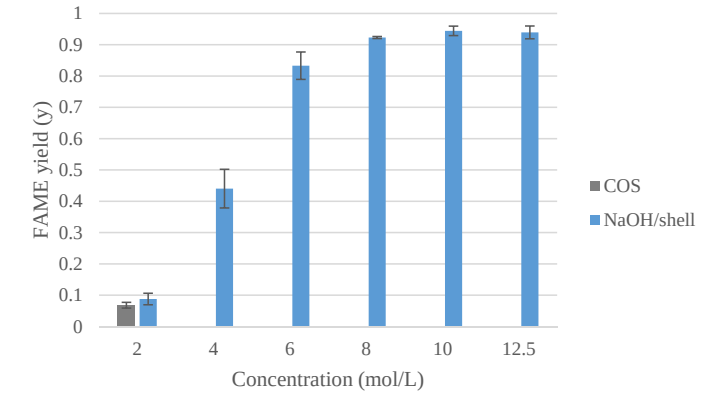

(**a**)

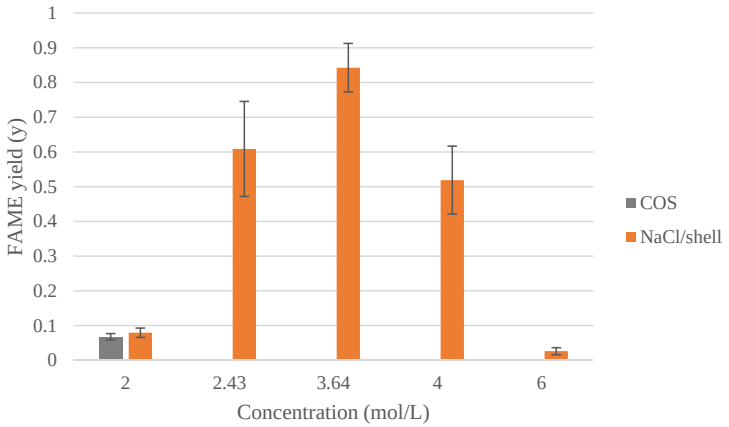

(**b**)

Figure 1. The FAME yield of the transesterification reaction catalyzed by various concentrations of NaOH (**a**) and NaCl (**b**) impregnated calcined oyster shell. Transesterification conditions: temperature = 62 °C; stirring rate = 800 rpm; MR = 12; CL = 10%.

However, for precursor concentrations beyond, 6 mol/L, FAME yields appeared to be similar (FAME yield between 83% and 94%) (Figure 1a). Our results agree with those reported by de Luna et al. who investigated the activity of NaOH impregnated pumice stone as catalysts for transesterification of soybean oil [17]. The authors reported a significant increase in fractional conversion of soybean oil when the precursor concentration was increased due to the incorporation of sodium ions within pumice stone matrix. The results obtained from NaCl/shell exhibited a different trend. As shown in Figure 1b, the FAME yield increased (from 8% to 84%) when the precursor concentration was increased from 2 mol/L to 3.64 mol/L and started decreasing when the precursor concentration was further increased beyond 3.64 mol/L, suggesting that presence of excess precursor may inhibit catalytic activity as shown in Figure 1. However, no significant differences in FAME yields were found between precursor loadings of 2.43 and 3.64 mol/L. Hence, precursor concentrations of 6 mol/L (for NaOH) and 2.43 mol/L (for NaCl) were selected for subsequent studies to investigate the effect of calcination of catalyst activity.

2.2. Effect of Calcination Temperature

The effects of calcination temperature are summarized in Figure 2. For experiments with NaOH/shell, calcination temperature (400, 600, 800, and 1000 °C) did not affect the yields of FAME that ranged between 80 and 91% (Figure 1a).

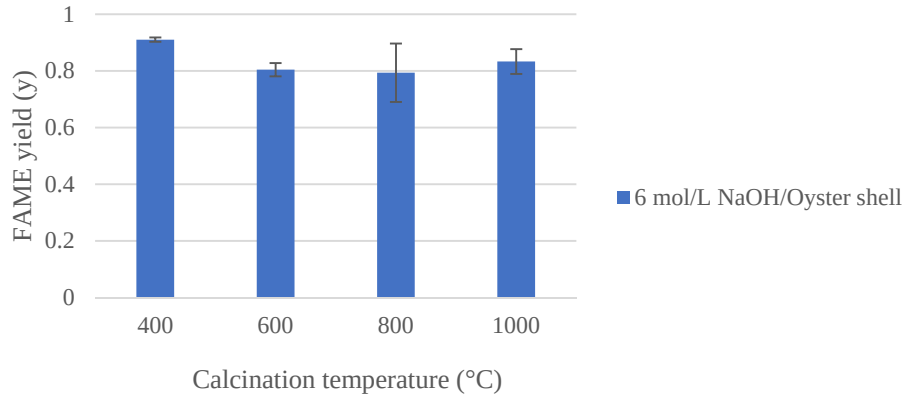

(**a**)

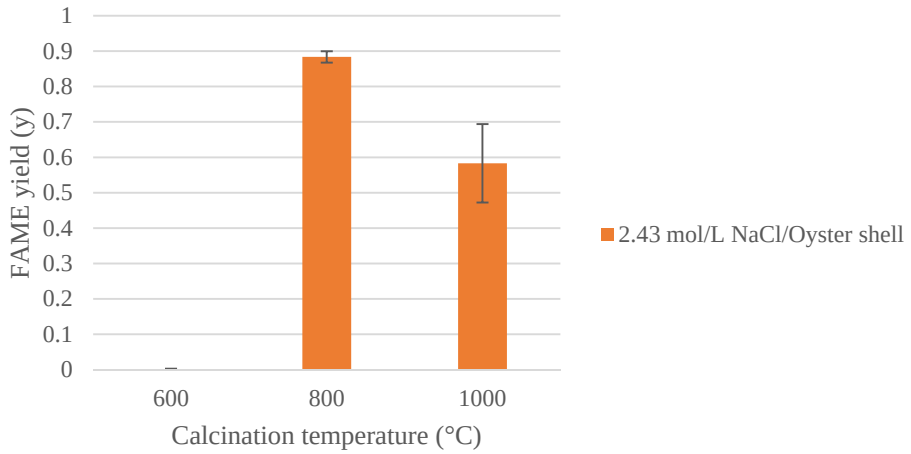

(**b**)

Figure 2. The FAME yield of the transesterification reaction catalyzed by $NaOH_6$/shell (**a**) and $NaCl_{2.43}$/shell (**b**) calcined at various temperatures. Transesterification conditions: temperature = 62 °C; stirring rate = 800 rpm; MR = 12; CL = 10%.

However, since the stability of catalyst depends on the calcination temperature, further experiments were conducted to evaluate the reusability of the catalysts calcined at all temperatures. The catalysts were reused consecutively for five times using fresh batches of methanol and oil to determine the yields of FAME. As shown in Figure 3, catalysts calcined at 400 °C started losing activity after the second run and provided a FAME yield of 26.2% after the fifth run. However, when calcination temperature was increased, the stability of the catalyst appeared to improve.

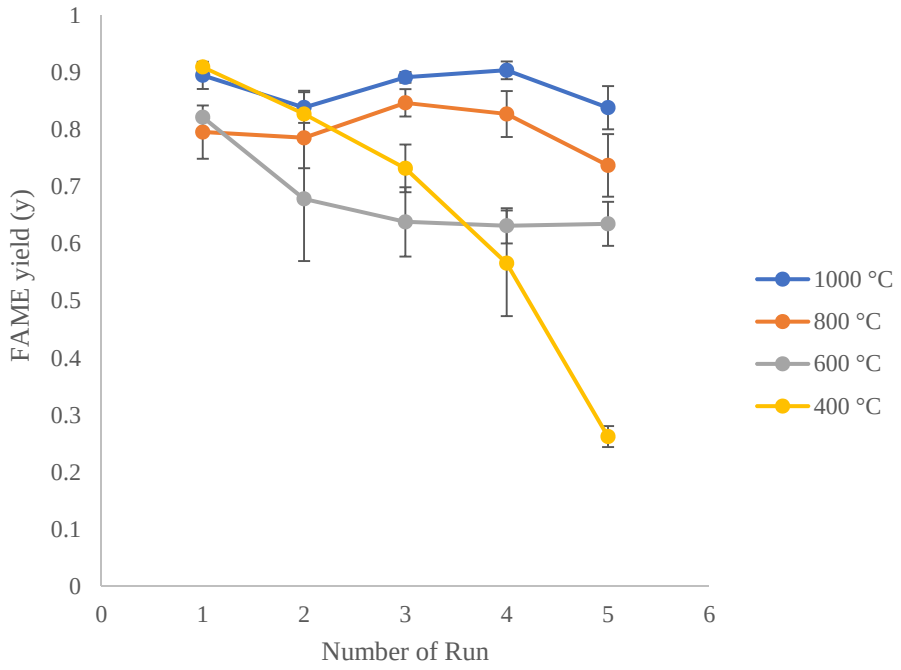

Figure 3. The FAME yield of repeated transesterifications reaction catalyzed by the same spent $NaOH_6$/shell calcined at various temperatures. Transesterification conditions: temperature = 62 °C; stirring rate = 800 rpm; MR = 12; CL = 10%.

The catalysts calcined at 800 and 1000 °C exhibited similar FAME yields for all five runs whereas the catalyst calcined at 600 °C provided lower FAME yields after the third run, when compared to 800 and 1000 °C suggesting that calcination at higher temperatures allowed for adequate reaction between Na ions and oyster shell resulting in strong binding of active sites on the surface.

For NaCl/shell, almost no activity was observed at 600 °C (FAME yield of ~0.1%) (Figure 2b). When the calcination temperature was increased to 800 °C the yield of FAME increased to 88.4% and started to decrease with an increase in calcination temperature beyond 800 °C.

Overall, it appears that NaOH/shell and NaCl/shell calcined at 800 °C provided best FAME yields and stability. Hence to elucidate the role of calcination and effects of precursor concentrations, the surface properties of catalysts synthesized under various conditions were studied in detail.

2.3. Catalyst Characterization

The specific surface areas and basicities of the catalysts synthesized are summarized in Table 1. The impregnation of NaOH or NaCl lowered the specific surface area of the oyster shell, probably because of deposition of precursor molecules within the pores of COS. Our results were similar to those noted by Alburquerque et al., who observed 90–98% reduction in surface area of SBA-15 support when 4–20% (*w*/*w*) CaO was impregnated [18]. Similarly, de Luna et al., impregnated NaOH on pumice stone to enhance its catalytic activity [17]. The authors reported a significant reduction in surface area and pore volume after impregnation due formation of active sites within the pores. In our research,

the basicity, however, showed no substantial difference between all types of catalysts, indicating that the precursor type and concentration calcination temperature did not alter the catalysts' basicity.

Table 1. The specific surface areas and basicities of COS, $NaOH_6$/shell-400, $NaOH_6$/shell-800, $NaCl_{2.43}$/shell-600, $NaCl_{2.43}$/shell-800 and $NaCl_{2.43}$/shell-1000.

Catalyst	Surface Area/m^2 g^{-1}	Basicity/mmol g^{-1}
COS	2.15	11.9
$NaOH_6$/shell-400	0.43	13.5
$NaOH_6$/shell-800	0.56	12.7
$NaCl_{2.43}$/shell-600	0.31	11.9
$NaCl_{2.43}$/shell-800	0.31	13.4
$NaCl_{2.43}$/shell-1000	0.69	13.3

The XRD pattern of each catalyst is shown in Figure 4a. For NaOH-impregnated shells, major phases formed on the surface of $NaOH_6$/shell-400 were $CaCO_3$, Na_2CO_3 and $Ca(OH)_2$. Since $CaCO_3$ and Na_2CO_3 are not catalytically very active for transesterification, it may be concluded that the catalytic activity of $NaOH_6$/shell-400 may be due to $Ca(OH)_2$. These results were similar to the results obtained by Kumar and Ali, who used KOH to modify the surface of CaO [19]. The as-synthesized nanocrystalline 3.5% K-CaO exhibited newly generated $Ca(OH)_2$ sites on the surface that contributed to the increased basic strength from 9.8< H_ <10.1 to 11.1< H_ <15.0. The activity was also improved as the FAME yield reached 98% in 75 min [19]. In our research, when the calcination temperature increased (from 400 °C to 800 °C), the type of surface species changed on the shells' surface. The major phases formed on the surface of $NaOH_6$/shell-800 were CaO and Na_2O_2, both of which are catalytically active in transesterification. The formation of alkaline oxide was also observed in the KNO_3 impregnated CaO-ZnO catalyst synthesized by Istabdi et al. [20]. The as-synthesized catalysts acquired K_2O on the surface, which might have resulted in the improved activity in the transesterification of soybean oil. A similar trend was observed in our research as well, in which, up to 90% FAME yields were obtained from the $NaOH_6$/shell-800 (Figure 1). It appeared that calcination at higher temperature allowed for decomposition of carbonate and hydroxide to respective oxides that are active and stable. In addition, as shown in the reusability experiments (Figure 3), $NaOH_6$/shell-800 provided high FAME yield even after five successive runs whereas the FAME yields for $NaOH_6$/shell-400 continually decreased to 26.2% after the fifth run, indicating a substantial loss of activity.

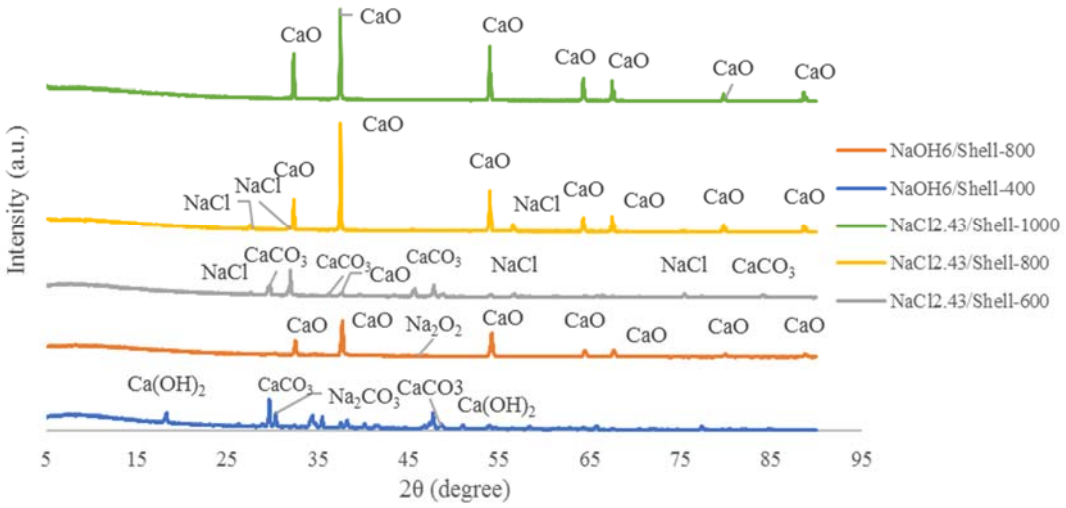

(**a**)

Figure 4. *Cont.*

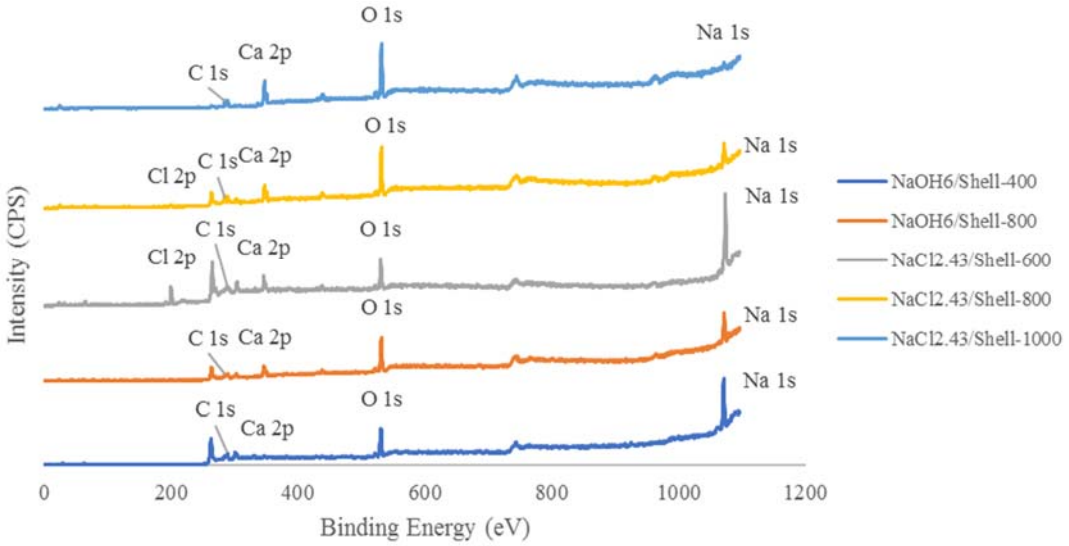

(**b**)

Figure 4. The XRD (**a**) and XPS (**b**) spectra of the sodium-supported oyster shell catalysts.

The XRD patterns of $NaCl_{2.43}$/shell-600, $NaCl_{2.43}$/shell-800 and $NaCl_{2.43}$/shell-1000 are also shown in Figure 4a. At 600 °C, the major phases identified were $CaCO_3$ and NaCl and traces of CaO. As a result, $NaCl_{2.43}$/shell-600 provided only 0.13% FAME yield after 2 h. When the calcination temperature increased to 800 °C, most $CaCO_3$ had been decomposed into CaO, resulting in the disappearance of $CaCO_3$ and increase in the intensity of CaO peaks as was also reported by Madhu et al. [21]. Because CaO is also an active catalyst, the FAME yield from $NaCl_{2.43}$/shell-800 increased up to 88.4%. Further increase in the calcination temperature to 1000 °C, however, decreased the yield to 58.3%. As seen from the XRD pattern for $NaCl_{2.43}$/shell-1000, only CaO was detected on the surface. The disappearance of NaCl in $NaCl_{2.43}$/shell-1000 might have caused the FAME yield to decrease. These results implied that a synergistic effect between NaCl and CaO on the surface of $NaCl_{2.43}$/shell-800 may have resulted in high FAME yields when compared to yields obtained from $NaCl_{2.43}$/shell-1000.

The XPS analyses of NaOH-impregnated catalysts indicated different elemental distribution for $NaOH_6$/shell-400 and $NaOH_6$/shell-800 catalysts (Figure 4b and Table 2). The atomic percentage of Na in $NaOH_6$/shell-400 was 42.6%, whereas the atomic percentage of Na dropped to 16.6% in $NaOH_6$/shell-800 as the calcination temperature increased from 400 to 800 °C. However, the atomic percentage of Ca in $NaOH_6$/shell-400 increased from 1.4% to 9.3% as the calcination temperature increased from 400 to 800 °C. Combined with the XRD results, the Na from the surface of $NaOH_6$/shell-400 probably originated from Na_2CO_3. When the calcination temperature increased, the Na_2CO_3 and $CaCO_3$ probably decomposed into Na_2O_2 and CaO as was revealed from XRD spectra.

Table 2. Composition and ratios of surface elements of NaOH/shell.

Temperature	C 1s	O 1s	Na 1s	Ca 2p	O/C	Na/C
400 °C	7.0%	49.0%	42.6%	1.4%	7.0	6.08
800 °C	29.3%	44.7%	16.6%	9.3%	1.52	0.56

Figure 5A presented the C 1s, Ca 2p, Na 1s, and O 1s regions for $NaOH_6$/Shell-400 and $NaOH_6$/Shell-800. In the C 1s region, both catalysts showed doublet peaks (285.0 eV and 289.2 eV for $NaOH_6$/Shell-400 and 285.0 eV and 289.5 eV for NaOH6/Shell-800), suggesting that they contained C-H and carbonate groups on the surface, probably from the air contamination [18]. In the Ca 2p region, $NaOH_6$/Shell-400 showed two peaks at 346.5 eV and 350.1 eV, suggesting that the Ca originated

from $CaCO_3$ [22]. $NaOH_6$/Shell-800 showed two peaks at 346.8 eV and 350.3 eV, suggesting that the Ca originated from CaO [23]. Similarly, in the Na 1s region, both catalysts displayed doublet peaks. In our analyses, the two peaks in both catalysts seemed to shift to lower BE by 1.0 eV compared with the references [24–26]. Combined with the details of the preparation method and the XRD results, the Na 1s peak at lower BE might have originated from Na_2CO_3, while the Na 1s peak at higher BE might be associated with NaOH and Na_2O_2 for $NaOH_6$/Shell-400 and $NaOH_6$/Shell-800, respectively [24–26]. In the O 1s region, $NaOH_6$/Shell-400 displayed doublet peaks at 530.3 eV and 531.2 eV, assigned to CaO and $Ca(OH)_2$, respectively [27,28]. Similarly, $NaOH_6$/Shell-800 exhibited doublet peaks at 530.3 eV and 531.5 eV, assigned to Na_2O_2 and CaO [29], respectively, based on the XRD analysis. This doublet feature indicated that some of the surface oxygen had been shifted to lower BE for both catalysts, when compared to control (calcined oyster shell), acquiring a higher effective negative charge. As was also observed in our recent research [16], the shift in oxygen would have enhanced the electron donating ability, suggesting that the surface oxygen was more basic [30]. As a result, the increased electron donating ability may have allowed triglyceride and methanol to form a tetrahedral intermediate that may have resulted in FAME after structural rearrangement [2].

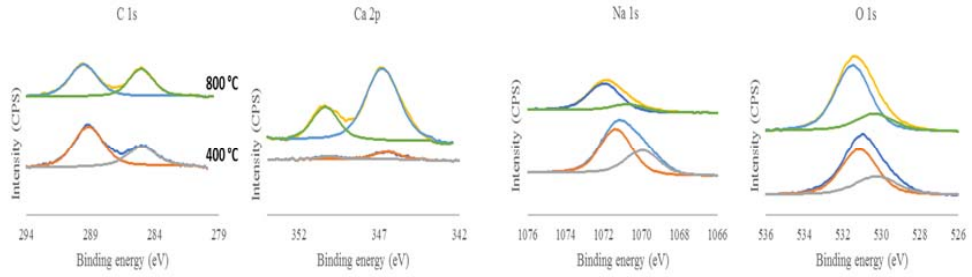

(**A**)

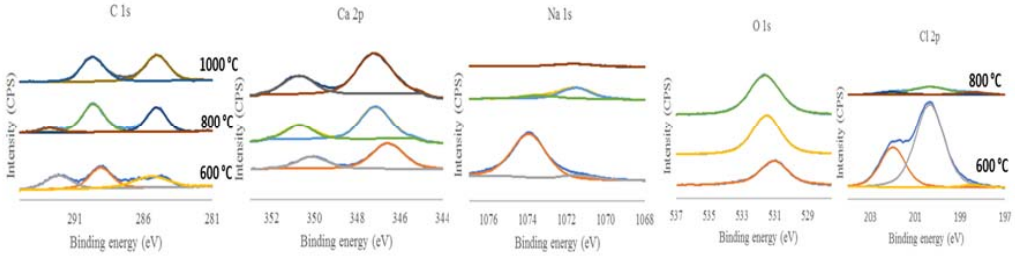

(**B**)

Figure 5. The elemental XPS peaks were deconvoluted for (**A**) NaOH supported oyster shell ($NaOH_6$/Shell-400 (bottom) and $NaOH_6$/Shell-800 (top) and (**B**) NaCl/Oyster shell ($NaCl_{2.43}$/Shell-600 (bottom), $NaCl_{2.43}$/Shell-800 (middle) and $NaCl_{2.43}$/Shell-1000 (top). For Cl 2p, $NaCl_{2.43}$/Shell-600 (bottom) and $NaCl_{2.43}$/Shell-800 (top)).

The XPS data obtained from NaCl-impregnated catalysts also revealed different elemental distributions for $NaCl_{2.43}$/shell-600, $NaCl_{2.43}$/shell-800, and $NaCl_{2.43}$/shell-1000 (Table 3). As the calcination temperature increased, the amount of Na and Cl decreased continuously from 32.4% (Na) and 15.0% (Cl) (for 600 °C calcination) to 10.0% and 2.1% (for 800 °C calcination), and finally dropped to 1.2% and 0% (for 1000 °C calcination), respectively, while the amount of Ca increased from 5.8% (600 °C) to 10.3% (800 °C), and finally reached 15.8% (1000 °C). These observations were consistent with the XRD results, in which the major phases of the catalyst, as the calcination temperature

increased, changed from carbonate to oxide for the Ca, and the intensity of NaCl phase was attenuated continuously and disappeared finally at 1000 °C.

Table 3. Composition and ratios of surface elements of NaCl/shell.

Temperature	C 1s	O 1s	Cl 2p	Na 1s	Ca 2p	O/C	Na/C
600 °C	22.5%	24.2%	15.0%	32.4%	5.8%	1.07	1.44
800 °C	32.1%	45.5%	2.1%	10.0%	10.3%	1.42	0.31
1000 °C	27.6%	55.4%	0%	1.2%	15.8%	2.00	0.04

Figure 5B presented the C 1s, Ca 2p, Na 1s, O 1s and Cl 2p regions for $NaCl_{2.43}$/Shell-600, $NaCl_{2.43}$/Shell-800 and $NaCl_{2.43}$/Shell-1000. In the C 1s region, $NaCl_{2.43}$/Shell-600 and $NaCl_{2.43}$/Shell-800 exhibited triplet peaks while $NaCl_{2.43}$/Shell-1000 showed doublet peaks. In addition to peaks at ~289.4 eV and ~285.0 eV (assigned to C-H and carbonate groups, respectively) [18], $NaCl_{2.43}$/Shell-600 and $NaCl_{2.43}$/Shell-800 also displayed a third C 1s peak at ~292.4 eV, which may be attributed to the existence of C-Cl [31]. $NaCl_{2.43}$/Shell-1000 did not contain Cl, and thus no such peak was detected. In the Ca 2p region, all three catalysts showed doublet peaks. The peaks at 346.6 eV and 350.1 eV in $NaCl_{2.43}$/Shell-600 were assigned to $CaCO_3$ [22]. The peaks at 347.1 eV and 350.6 eV in $NaCl_{2.43}$/Shell-800 and at 347.2 eV and 350.7 eV in $NaCl_{2.43}$/Shell-1000 were assigned to CaO [29]. In the Na region, $NaCl_{2.43}$/Shell-600 and $NaCl_{2.43}$/Shell-800 displayed doublet peaks at ~1073.6 eV and ~1071.5 eV, assigned to NaCl [32] and Na_2CO_3 [25], respectively, while $NaCl_{2.43}$/Shell-1000 only showed single peak at 1071.6 eV, assigned to Na_2CO_3 [25]. The Na_2CO_3 in $NaCl_{2.43}$/Shell-600 may be attributed to adsorbed Na and undecomposed carbonate in the shell matrix, while the Na_2CO_3 in $NaCl_{2.43}$/Shell-800 and $NaCl_{2.43}$/Shell-1000 might be attributed to the air contaminant on the surface since no carbonate group was detected based on the XRD analysis. Because $NaCl_{2.43}$/Shell-1000 did not contain Cl, it did not exhibit a peak representing NaCl. In the O 1s region, all three catalysts exhibited a single peak. The peak at 531.0 eV of $NaCl_{2.43}$/Shell-600 was assigned to $CaCO_3$ [23] and the peak at 531.5 eV of $NaCl_{2.43}$/Shell-800 and the peak at 531.6 eV of $NaCl_{2.43}$/Shell-1000 were assigned to CaO [29]. In the Cl 2p region, both $NaCl_{2.43}$/Shell-600 and $NaCl_{2.43}$/Shell-800 displayed doublet peaks at 200.3 eV and 202.0 eV, for 2p3/2 and 2p1/2 components of Cl, respectively, with a separation of 1.7 eV that was also observed by Wu et al. [33]. In addition, $NaCl_{2.43}$/Shell-800 also had a third peak at lower BE, 198.4 eV. Comparing the FAME yields of $NaCl_{2.43}$/Shell-800 with $NaCl_{2.43}$/Shell-1000 indicated that $NaCl_{2.43}$/Shell-800 resulted in higher FAME yield than $NaCl_{2.43}$/Shell-1000. Considering that the BE of O 1s for $NaCl_{2.43}$/Shell-800 was comparable with $NaCl_{2.43}$/Shell-1000, the enhanced activity of $NaCl_{2.43}$/Shell-800 may have been due to the formation of surface Cl with lower BE (198.4 eV). As shown in Figure 6, the negatively shifted Cl probably behaved similarly as the negatively shifted O, thereby increasing the effective negative charge that led to an increase in the electron donating ability and enhanced the FAME production rate by facilitating the formation of the tetrahedral intermediate between adsorbed triglyceride and methanol [2,30]. This synergistic effect between NaCl and CaO appears to have occurred at 800 °C because the catalysts calcined at 600 °C and 100 °C did not exhibit high activity despite equipped with identical NaCl loading.

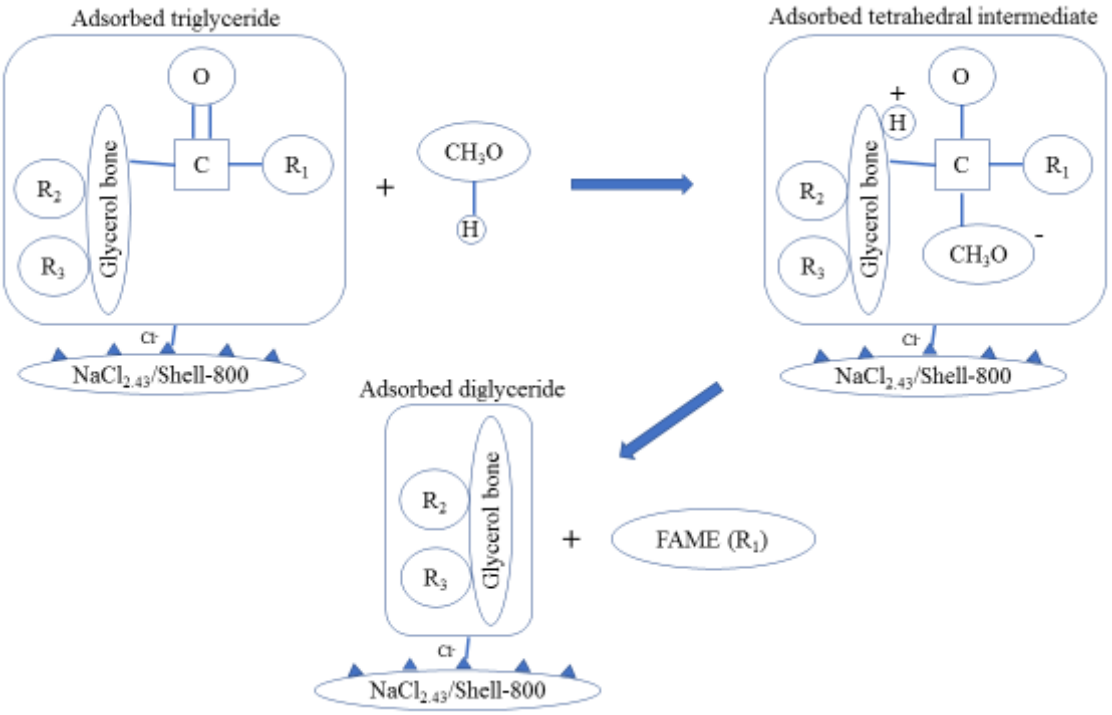

Figure 6. Role of $NaCl_{2.43}$/Shell-800 surface basic site on the improved activity.

3. Materials and Methods

3.1. Catalyst Preparation

Discarded oyster shells were procured locally. The dirt on the shells were cleaned in running water and allowed to dry overnight. Subsequently, the shells were calcined (2h @ 500 °C) and crushed (1–2 mm).

Two types of Na-based precursor solutions were employed in this research: NaOH and NaCl. Typically, 20 g of oyster shells were impregnated with 60 mL of precursor solutions (90 °C for 5 h) of predetermined concentration on a process-controlled hot plate (Isotemp, Fisher Scientific, Pittsburgh, PA). Subsequently, the impregnated shells were filtered and calcined at a predetermined temperature for 3 h (with a flow of nitrogen).

3.2. Catalyst Characterization

The specific surface area of the catalyst synthesized was determined using Quantachrome Monosorb Surface Area Analyzer (Quantachrome Instruments, Boynton Beach, FL, USA) based on the Brunauer–Emmett–Teller (BET) nitrogen adsorption method [16]. Prior to the measurement, all catalysts were degassed at 120 °C for 8 h.

The basicity of the catalyst was determined as described by Mo et al. [34]. 0.1 g sample was soaked into 20 mL of the 0.1 N HCl solution for 20 min flowed by titration using 0.15 N NaOH with Phenolphthalein.

X-ray powder diffraction (XRD) analyses were performed via a PANalytical Empyrean X-ray diffractometer (Malvern Panalytical Ltd., Almelo, Netherlands) with Cu Kα radiation (λ = 0.15418 nm) in the 2θ range of 5°–90°. The data were collected as described previously [16].

The samples were also analyzed via X-ray photoelectron spectroscopy (XPS) using a SPECS FlexMod system (SPECS GmbH, Berlin, Germany) equipped with a hemispherical analyzer PHOIBIS 150 and a Mg Kalpha (1254 eV) X-ray source @ 10^{-10} mbar) using adventitious Carbon (C 1s line at 285.0 eV binding energy) as reference.

3.3. Transesterification

Batch experiments were performed (in duplicates) 250 mL three-neck glass reactors. 20 mL of soybean oil was reacted (62 °C and 800 rpm) with predetermined amount of methanol and catalyst on a process-controlled hot plate (Isotemp, Fisher Scientific, Pittsburgh, PA, USA). In this research, the molar ratio of methanol to oil (MR) and catalyst loading (CL) were set to 12 and 10%, respectively. After a 2-h reaction, 3 mL of the reaction mixture was transferred to 15 mL plastic tubes for centrifugation (5000 rpm for 5 min) to remove the catalyst. Subsequently, 800 µL of the supernatant liquid was drawn and washed three times with DI water from which a 300 µL sample was collected for further gas chromatographic analysis.

3.4. Gas Chromatography Analysis

A gas chromatograph with a mass spectrometer (Agilent 7890/5975C) was used to separate, detect, and quantify FAME using Methyl Laurate (99% purity, CAS 111-82-0) as an internal standard as described in Jin et al., (2017b). FAME yields were calculated using the equation below, as proposed by Liu et al and Chung et al [2,35].

$$\text{Yield} = \frac{(\sum A)-A_{IS}}{A_{IS}} \times \frac{C_{IS}V}{m_{FAMEs}} \times 100\% \approx \frac{(\sum A)-A_{IS}}{A_{IS}} \times \frac{C_{IS}V}{m_{oil}} \times 100\% = \frac{(\sum A)-A_{IS}}{A_{IS}} \times \frac{C_{IS}\times V}{\rho_{oil}\times\frac{1}{r}\times V} \times 100\% = \frac{(\sum A)-A_{IS}}{A_{IS}} \times \frac{C_{IS}}{C_{oil}} \times 100\%$$

where $\sum A$ is the total area of peak areas of all methyl esters, A_{IS} is the peak area of Methyl Laurate, C_{IS} is the concentration of Methyl Laurate in the solution after dilution (g/mL), V is the volume of the final diluted solution (mL), m_{FAMEs} is the theoretical maximum mass of FAMEs (g), m_{oil} is the mass of pure soybean oil of volume V (g), ρ_{oil} is the density of soybean oil (g/mL), r is the dilution ratio of FAMEs sample, C_{oil} is the corresponding concentration of soybean oil (g/mL) in the solution after dilution, if dilution ratio is r.

3.5. Experimental Design

All experiments were performed in duplicates. For the synthesis of NaCl/shell catalyst, NaCl solutions of 2, 2.43, 3.64, 4, and 6 mol/L were employed. Similarly, for the synthesis of NaOH/shell catalyst, NaOH solutions of 2, 4, 6, 8, 10, and 12.5 were used. All catalysts synthesized were tested in batch reactors and the FAME yields were analyzed using SAS (SAS Institute Inc., Cary, NC, USA).

The optimal conditions of each precursor type were chosen based on the FAME yield. The corresponding catalyst was then re-prepared but calcined at various temperatures. For NaCl-impregnated catalysts, calcination temperatures of 600 °C, 800 °C, 1000 °C and for NaOH-impregnated catalysts, calcination temperatures of 400 °C, 600 °C, 800 °C, and 1000 °C were used.

Additional experiments were performed to test the reusability of the various NaOH-impregnated calcined oyster shells. The spent catalyst was used for five consecutive runs. After each run, the FAME yield was determined and the recovered catalyst was applied to subsequent run without any treatment. The data were analyzed via a Tukey's HSD test.

4. Conclusions

This research investigated how preparation conditions affected the structure and activity of transesterification catalysts derived from waste oyster shells. Oyster shells that were impregnated with various concentrations of NaOH and NaCl and calcined at different temperatures were tested as catalysts in batch experiments. Based on results obtained from batch experiments and catalyst characterization, it appears that precursor type and calcination temperature determined the formation of newly generated surface species that influenced the activity of the catalyst. In general, higher

calcination temperature converted more carbonates and hydroxides into oxides that enhanced catalyst activity due to a higher electron donating ability.

Author Contributions: H.J. designed and conducted the experiments, performed the data analysis, and wrote the manuscript; P.K. conceived the idea, supervised the research and edited the manuscript; J.J.C. and S.W.P. contributed to the catalyst characterization and reaction mechanisms of the transesterification reaction. J.A.O. contributed to the experimental design and data analysis.

Acknowledgments: The authors thank Chung, Fred Stevie, Andrew Whitaker, and Maia Fitzstevens for the help on catalyst characterization, Tu for the help on the experiment supplies and Department of Biological and Agricultural Engineering for funding support. This work was performed in part at the Analytical Instrumentation Facility (AIF) at North Carolina State University, which is supported by the State of North Carolina and the National Science Foundation (award number ECCS-1542015). The AIF is a member of the North Carolina Research Triangle Nanotechnology Network (RTNN), a site in the National Nanotechnology Coordinated Infrastructure (NNCI).

Conflicts of Interest: The authors declare no conflict of interest.

References

1. Kawashima, A.; Matsubara, K.; Honda, K. Development of heterogeneous base catalysts for biodiesel production. *Bioresour. Technol.* **2008**, *99*, 3439–3443. [CrossRef] [PubMed]
2. Liu, X.; He, H.; Wang, Y.; Zhu, S.; Piao, X. Transesterification of soybean oil to biodiesel using CaO as a solid base catalyst. *Fuel* **2008**, *87*, 216–221. [CrossRef]
3. Meher, L.C.; Kulkarni, M.G.; Dalai, A.K.; Naik, S.N. Transesterification of karanja (*Pongamia pinnata*) oil by solid basic catalysts. *Eur. J. Lipid Sci. Technol.* **2006**, *108*, 389–397. [CrossRef]
4. Watkins, R.S.; Lee, A.F.; Wilson, K. Li–CaO catalysed tri-glyceride transesterification for biodiesel applications. *Green Chem.* **2004**, *6*, 335–340. [CrossRef]
5. Mar, W.W.; Somsook, E. Methanolysis of soybean oil over KCl/CaO solid base catalyst for biodiesel production. *Sci. Asia* **2012**, *38*, 90–94. [CrossRef]
6. Wen, L.; Wang, Y.; Lu, D.; Hu, S.; Han, H. Preparation of KF/CaO nanocatalyst and its application in biodiesel production from Chinese tallow seed oil. *Fuel* **2010**, *89*, 2267–2271. [CrossRef]
7. Liu, C.C.; Lu, W.C.; Liu, T.J. Transesterification of soybean oil using CsF/CaO catalysts. *Energy Fuels* **2012**, *26*, 5400–5407. [CrossRef]
8. Mahesh, S.E.; Ramanathan, A.; Begum, K.M.M.S.; Narayanan, A. Biodiesel production from waste cooking oil using KBr impregnated CaO as catalyst. *Energy Convers. Manag.* **2015**, *91*, 442–450. [CrossRef]
9. Yan, S.; Kim, M.; Mohan, S.; Salley, S.O.; Ng, K.Y.S. Effects of preparative parameters on the structure and performance of Ca-La metal oxide catalysts for oil transesterification. *Appl. Catal. A Gen.* **2010**, *373*, 104–111. [CrossRef]
10. Kaur, N.; Ali, A. Kinetics and reusability of Zr/CaO as heterogeneous catalyst for the ethanolysis and methanolysis of *Jatropha crucas* oil. *Fuel Process. Technol.* **2014**, *119*, 173–184. [CrossRef]
11. Wei, Z.; Xu, C.; Li, B. Application of waste eggshell as low-cost solid catalyst for biodiesel production. *Bioresour. Technol.* **2009**, *100*, 2883–2885. [CrossRef] [PubMed]
12. Rezaei, R.; Mohadesi, M.; Moradi, G.R. Optimization of biodiesel production using waste mussel shell catalyst. *Fuel* **2013**, *109*, 534–541. [CrossRef]
13. Suryaputra, W.; Winata, I.; Indraswati, N.; Ismadji, S. Waste capiz (*Amusium cristatum*) shell as a new heterogeneous catalyst for biodiesel production. *Renew. Energy* **2013**, *50*, 795–799. [CrossRef]
14. Jairam, S.; Kolar, P.; Sharma-Shivappa Ratna, R.; Osborne, J.A.; Davis, J.P. KI-impregnated oyster shell as a solid catalyst for soybean oil transesterification. *Bioresour. Technol.* **2012**, *104*, 329–335. [CrossRef] [PubMed]
15. Jin, H.; Kolar, P.; Peretti, S.W.; Osborne, J.A.; Cheng, J.J. NaOH-impregnated oyster shell as a solid base catalyst for transesterification of soybean oil. *Int. J. Agric. Biol. Eng.* **2017**. accepted.
16. Jin, H.; Kolar, P.; Peretti, S.W.; Osborne, J.A.; Cheng, J.J. Kinetics and mechanism of NaOH-impregnated calcined oyster shell-catalyzed transesterification of soybean oil. *Energies* **2017**, *10*, 1920. [CrossRef]
17. De Luna, M.D.G.; Cuasay, J.L.; Tolosa, N.C.; Chung, T.W. Transesterification of soybean oil using a novel heterogeneous base catalyst: Synthesis and characterization of Na-pumice catalyst, optimization of

transesterification conditions, studies on reaction kinetics and catalyst reusability. *Fuel* **2017**, *209*, 246–253. [CrossRef]
18. Albuquerque, M.C.G.; Jiménez-Urbistondo, I.; Santamaría-González, J.; Mérida-Robles, J.M.; Moreno-Tost, R.; Rodríguez-Castellón, E.; Jiménez-López, A.; Azevedo, D.C.S.; Cavalcante, C.L.; Maireles-Torres, P. CaO supported on mesoporous silicas as basic catalysts for transesterification reactions. *Appl. Catal. A Gen.* **2008**, *334*, 35–43. [CrossRef]
19. Kumar, D.; Ali, A. Nanocrystalline K-CaO for the transesterification of a variety of feedstocks: Structure, kinetics and catalytic properties. *Biomass Bioenergy* **2012**, *46*, 459–468. [CrossRef]
20. Istadi, I.; Prasetyo, S.A.; Nugroho, T.S. Characterization of K_2O/CaO-ZnO Catalyst for Transesterification of Soybean Oil to Biodiesel. *Procedia Environ. Sci.* **2015**, *23*, 394–399. [CrossRef]
21. Madhu, D.; Chavan, S.B.; Singh, V.; Singh, B.; Sharma, Y.C. An economically viable synthesis of biodiesel from a crude *Millettia pinnata* oil of Jharkhand, India as feedstock and crab shell derived catalyst. *Bioresour. Technol.* **2016**, *214*, 210–217. [CrossRef] [PubMed]
22. Ni, M.; Ratner, B.D. Differentiating calcium carbonate polymorphs by surface analysis techniques—An XPS and TOF-SIMS study. *Surf. Interface Anal.* **2008**, *40*, 1356–1361. [CrossRef] [PubMed]
23. Demri, B.; Muster, D. XPS study of some calcium compounds. *J. Mater. Process. Technol.* **1995**, *55*, 311–314. [CrossRef]
24. Hammond, J.S.; Holubka, J.W.; deVries, J.E.; Dickie, R.A. The application of x-ray photo-electron spectroscopy to a study of interfacial composition in corrosion-induced paint de-adhesion. *Corros. Sci.* **1981**, *21*, 239–253. [CrossRef]
25. Siriwardane, R.V.; Cook, J.M. Interactions of NO and SO_2 with iron deposited on silica. *J. Colloid Interface Sci.* **1985**, *104*, 250–257. [CrossRef]
26. Wu, Q.H.; Thißen, A.; Jaegermann, W. XPS and UPS study of Na deposition on thin film V_2O_5. *Appl. Surf. Sci.* **2005**, *252*, 1801–1805. [CrossRef]
27. Van Doveren, H.; Verhoeven, J.A.T.H. XPS spectra of Ca, Sr, Ba and their oxides. *J. Electron Spectrosc. Relat. Phenom.* **1980**, *21*, 265–273. [CrossRef]
28. Sugama, T.; Kukacka, L.E.; Carciello, N.; Hocker, N.J. Study of interactions at water-soluble polymer/$Ca(OH)_2$ or gibbsite interfaces by XPS. *Cem. Concr. Res.* **1989**, *19*, 857–867. [CrossRef]
29. Hanawa, T.; Ota, M. Calcium phosphate naturally formed on titanium in electrolyte solution. *Biomaterials* **1991**, *12*, 767–774. [CrossRef]
30. Babu, N.S.; Sree, R.; Prasad, P.S.S.; Lingaiah, N. Room-temperature transesterification of edible and nonedible oils using a heterogeneous strong basic Mg/La catalyst. *Energy Fuels* **2008**, *22*, 1965–1971. [CrossRef]
31. Gelius, U.; Hedén, P.F.; Hedman, J.; Lindberg, B.J.; Manne, R.; Nordberg, R.; Nordling, C.; Siegbahn, K. Molecular Spectroscopy by Means of ESCA: III Carbon Compounds. *Phys. Scr.* **1970**, *2*, 70–80. [CrossRef]
32. Kishi, K.; Kirimura, H.; Fujimoto, Y. XPS studies for NaCl deposited on the Ni(111) surface. *Surf. Sci.* **1987**, *181*, 586–595. [CrossRef]
33. Wu, J.; Li, W.; Fortner, J.D. Photoenhanced oxidation of C_{60} aggregates (nC_{60}) by free chlorine in water. *Environ. Sci. Nano* **2017**, *4*, 117–126. [CrossRef]
34. Mo, X.; López, D.E.; Suwannakarn, K.; Liu, Y.; Lotero, E.; Goodwin, J.G.; Lu, C. Activation and deactivation characteristics of sulfonated carbon catalysts. *J. Catal.* **2008**, *254*, 332–338. [CrossRef]
35. Chung, K.H.; Kim, J.; Lee, K.Y. Biodiesel production by transesterification of duck tallow with methanol on alkali catalysts. *Biomass Bioenergy* **2009**, *33*, 155–158. [CrossRef]